Deep-Sea Research II 58 (2011) 664–677

Contents lists available at ScienceDirect

Deep-Sea Research II

journal homepage: www.elsevier.com/locate/dsr2

Characterisation of water masses and phytoplankton nutrient limitation in the East Australian Current separation zone during spring 2008

C.S. Hassler [a,b,c,*], J.R. Djajadikarta [c], M.A. Doblin [c], J.D. Everett [d], P.A. Thompson [b,e]

[a] Center for Australian Weather and Climate Research (CAWCR), a partnership between CSIRO and the Bureau of Meteorology. Castray Esplanade, Hobart TAS 7000, Australia
[b] Wealth from Oceans, National Research Flagship
[c] Plant Functional Biology and Climate Change Cluster, Faculty of Science, University of Technology, Sydney, P.O. Box 123, Broadway NSW 2007, Australia
[d] School of Biological Earth and Environmental Sciences, University of New South Wales, Sydney NSW 2052, Australia
[e] CSIRO Wealth from Oceans, National Research Flagship, Castray Esplanade, Hobart TAS 7000, Australia

ARTICLE INFO

Article history:
Received 15 June 2010
Accepted 15 June 2010
Available online 26 June 2010

Keywords:
Phytoplankton
Nutrient limitation
East Australian Current
Eddy

ABSTRACT

This study focuses on the comparison of oceanic and coastal cold-core eddies with inner-shelf and East Australian Current (EAC) waters at the time of the spring bloom (October 2008). The surface water was biologically characterised by the phytoplankton biomass, composition, photo-physiology, carbon fixation and by nutrient-enrichment experiments. Marked differences in phytoplankton biomass and composition were observed. Contrasted biomarker composition suggests that biomarkers could be used to track water masses in this area. Divinyl chlorophyll *a*, a biomarker for tropical Prochlorophytes, was found only in the EAC. Zeaxanthin a biomarker for Cyanophytes, was found only within the oceanic eddy and in the EAC, whereas chlorophyll *b* (Chlorophytes) was only present in the coastal eddy and at the front between the inner-shelf and EAC waters.

This study showed that cold-core eddies can affect phytoplankton, biomass, biodiversity and productivity. Inside the oceanic eddy, greater phytoplankton biomass and a more complex phytoplankton community were observed relative to adjacent water masses (including the EAC). In fact, phytoplankton communities inside the oceanic eddy more closely resembled the community observed in the inner-shelf waters. At a light level close to half-saturation, phytoplankton carbon fixation (gC d^{-1}) in the oceanic eddy was 13-times greater than at the frontal zone between the eddy and the EAC and 3-times greater than in the inner-shelf water. Nutrient-enrichment experiments demonstrated that nitrogen was the major macronutrient limiting phytoplankton growth in water masses associated with the oceanic eddy. Although the effective quantum yield values demonstrate healthy phytoplankton communities, the phytoplankton community bloomed and shifted in response to nitrogen enrichments inside the oceanic eddy and in the frontal zone between this eddy and the EAC. An effect of Si enrichment was only observed at the frontal zone between the eddy and the EAC. No response to nutrient enrichment was observed in the inner-shelf water where ambient NO_x, Si and PO_4 concentrations were up to 14, 4 and 3-times greater than in the EAC and oceanic eddy. Although results from the nutrient-enrichment experiments suggest that nutrients can affect biomass and the composition of the phytoplankton community, the comparison of all sites sampled showed no direct relationship between phytoplankton biomass, nutrients and the depth of the mixed layer. This is probably due to the different timeframe between the rapidly changing physical and chemical oceanography in the separation zone of the EAC.

1. Introduction

Biogeochemical properties of water masses along the coast of south east Australia are dominated by the presence of the East Australian Current (EAC, Nilsson and Cresswell, 1981). The EAC is a complex and highly variable western boundary current, with a summer flow (16 Sv) twice as strong as in winter (7 Sv; Godfrey et al., 1980b, Ridgway and Godfrey, 1997). Extending from the Coral Sea to the Tasman Sea, the EAC advects warm oligotrophic Coral seawater and its resident organisms southwards along the offshore edge of the continental shelf (Booth et al., 2007; Baird et al., 2008; Thompson et al., 2009).

The EAC tends to separate from the coast between 30 and 34°S (Godfrey et al., 1980b), with up to one-third of the EAC continuing southwards into the Tasman Sea (Tilburg et al., 2001). In this

* Corresponding author at: Plant Functional Biology and Climate Change Cluster, Faculty of Science, University of Technology, Sydney, P.O. Box 123, Broadway 2007, NSW, Australia. Tel.: +2 95 14 41 59; fax: +2 95 14 40 79.
E-mail address: Christel.Hassler@uts.edu.au (C.S. Hassler).

0967-0645/$ - see front matter © 2010 Elsevier Ltd. All rights reserved.
doi:10.1016/j.dsr2.2010.06.008

region, the continental shelf narrows, forcing the EAC to accelerate and turn away from the coast (Oke and Middleton, 2000). This acceleration and separation result in uplift of nutrient-rich slope water onto the continental shelf (Tranter et al., 1986; McLean-Padman and Padman, 1991; Roughan and Middleton, 2002, 2004), generating marked upwelling signatures in sea-surface temperature (SST), nutrients and chlorophyll *a* (Oke and Middleton, 2001). This coastal region is known as "the separation zone", from where the EAC meanders eastward across the Tasman Sea, leaving behind a dynamic southward moving eddy field (Godfrey et al., 1980b; Ridgway and Godfrey, 1997).

The water mass properties in this separation zone are thus highly variable, resulting from the EAC intrusion onto the continental shelf, the entrainment of upwelled and inner-shelf waters (Tranter et al., 1986; Cresswell, 1994) and the formation of mesoscale eddies (Godfrey et al., 1980b; Ridgway and Godfrey, 1997). The EAC separation zone therefore represents a convergence of numerous water masses, each of which has different characteristics of salinity, temperature, dissolved nutrients and mixed-layer depth; factors that influence biological properties such as the distribution and ecology of phytoplankton as well as primary productivity (e.g., Bakun, 2006; Baird et al., 2008 for the Tasman frontal zone resulting from the EAC separation zone).

Although regional circulation models (Baird et al., 2006) and recently applied underwater autonomous vehicles have helped resolve the complexity of chemical and physical oceanography in this region (Baird et al., 2011), there has been no analysis of phytoplankton biodiversity and productivity in the EAC separation zone since the 1990s (e.g., Jeffrey and Hallegraeff, 1980). Phytoplankton in the region are dominated by nanoflagellates (cells <15 μm in diameter) including prymnesiophytes, prasinophytes and dinoflagellates, with episodic, short-lived blooms of chain-forming diatoms >15 μm (Hallegraeff, 1981). There is no clear seasonal variation in species composition, but blooms occur in spring and autumn (September–October and February–March, respectively) as well as summer, and involve a sequence from small chain-forming species to large centric species and eventually to large dinoflagellates (Newell, 1996; Hallegraeff and Reid, 1996). Such blooms are widespread along the NSW coastline and are the result of nutrient-rich continental slope water intruding onto the shelf due to the EAC and its associated eddies (Tranter et al., 1986; Hallegraeff and Jeffrey, 1993). Warm-core eddies that pinch off from the meandering EAC show a more diverse community at their edge and slight elevation of phytoplankton biomass in their centre (Jeffrey and Hallegraeff, 1980) and can result in a mixture of temperate and tropical species in NSW shelf waters (Hallegraeff and Reid, 1986).

Although the mechanisms for nutrient enrichment of surface waters are well understood (Oke and Middleton, 2000, 2001; Roughan and Middleton, 2002), little is known about nutrient limitation of phytoplankton growth and its effect on productivity in the NSW region. In view of the long-term decline in silicate concentrations at Port Hacking (Thompson et al., 2009), and the observed intensification of EAC flow and its greater southwards intrusion (Ridgway and Hill, 2009), investigating the links between physical oceanography, nutrients and phytoplankton abundance, biodiversity and productivity in this area is urgently required.

This study tests the hypothesis that variable water masses in the EAC separation zone result in characteristic and demonstrably unique phytoplankton communities and productivity. This work compares oceanic and coastal cold-core eddies with inner-shelf and EAC waters in the late stage of the spring bloom (October 2008). The water masses were biologically characterised by determining phytoplankton biomass, composition, photo-physiology and carbon fixation. Nutrient-enrichment experiments were used to determine which nutrient (nitrate, phosphate or silicate), limited the biomass, productivity and biodiversity of natural phytoplankton communities present in the area.

2. Methods

2.1. Study region

The cruise aboard the *R.V. Southern Surveyor* took place during the Austral spring, from 10 to 20 October 2008. Prior to the cruise, in mid-September 2008, the EAC had relatively weak flow, with an average temperature range between 20 and 22 °C and a significant retroflection around 35°S (as determined by satellite imagery, Legacy Bureau of Meterology SST, not shown in Fig. 1 A). By the commencement of sampling in October, 2008, the EAC core had warmed to 23 °C (Fig. 1A). There was a $\sim$6 °C temperature difference across the interface of Coral Sea and Tasman Sea waters, indicating a strong Tasman Front (Baird et al., 2008). The EAC temperature during this time was approximately 1–2 °C warmer than the average October SST over the previous 50 years (from CSIRO Atlas of Regional Seas (CARS), version 2006a).

The surveyed area extended from Diamond Head (31°44′S) in the north to Sydney (34°S) in the south. Eight stations representing contrasting water masses were sampled along four different transects running parallel or perpendicular to the coast (Fig. 1). Water masses were identified using satellite data from the Moderate Resolution Imaging Spectroradiometer (MODIS) and Advanced Very High Resolution Radiometer (AVHRR), and were confirmed *in situ* using the CSIRO undulating towed device called the Bunyip (a highly modified SeaSoar) and the onboard Acoustic Doppler Current Profiler (data not presented here). A large 120-km diameter oceanic cyclonic (cold-core) eddy was sampled on 11 and 12 October 2008 (Stations 1 and 2). Satellite imagery (LBoMSST) indicated this eddy formed approximately two months prior to sampling and was made up of Tasman seawater that had been 'spun-up" by the adjacent EAC. Station 3 was located in the frontal zone between the EAC and the oceanic eddy and station 4 in the EAC. A small 40-km-diameter cyclonic eddy was also sampled on the 15 October 2008 (Station 5). This eddy formed on the inner-shelf at 33°S 152.5°E between 10 and 12 October 2008 (Table 1) and was created from an upwelled filament of cold water off Seal Rocks and by 15 October had been advected south by the adjacent EAC to 34°S 152°E, where the Sydney transect (Stations 4–6) bisected it (Fig. 1). Another transect (Stations 7–8) of inner-shelf water was sampled off Broken Bay on 17 October.

2.2. CTD transects and water sampling

Transects provided a quasi-synoptic view of the meso-scale physical and biological structure of the study region. Conductivity, temperature, depth, salinity and fluorescence profiles (0–300 m) were recorded electronically (Seabird SBE 911) at intervals of 1 m depth at each site. CTD casts within a transect were spaced approximately 4–6 nautical miles apart. Water samples were collected using 10-L Niskin bottles on the CTD rosette at eight nominal depths ranging from 0 to 300 m (5, 25, 50, 75, 100, 150, 200 and 300 m). Depths were adjusted to capture the fluorescence maximum as indicated on the downcast profile. The water collected was used for measurements of macronutrients (NO_x, Si, PO_4), dissolved oxygen and salinity. Profiles of down-welling irradiance (PAR) were made with a Biospherical Instruments QCP-2300 Log Quantum Cosine Irradiance Sensor. Hydrochemical analyses were carried out on board by CSIRO Marine and Atmospheric Research (CMAR) according to Cowley et al. (1999).

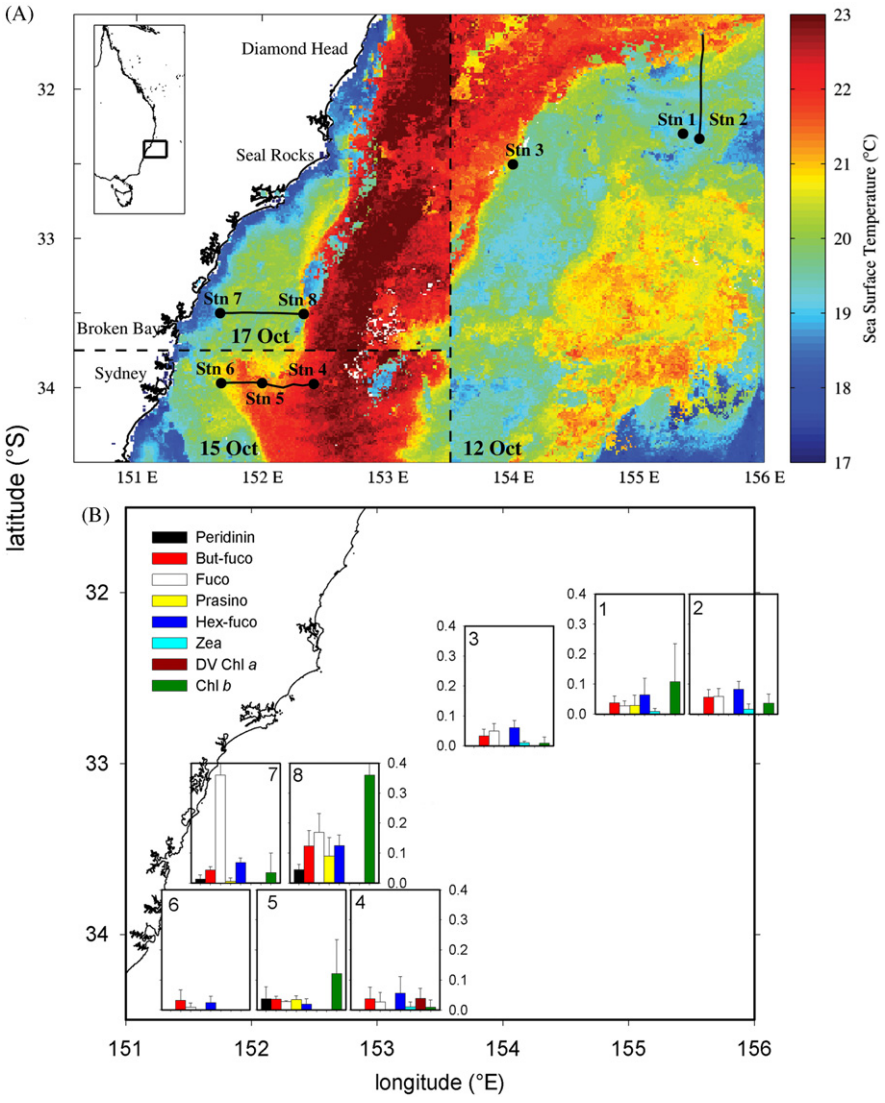

Fig. 1. Map of study area and sea-surface temperature (SST; A). Dashed lines bound the SST conditions for each day of sampling, as indicated by the date. Stations are shown as black circles. The entire CTD transects are shown as black lines. SST is derived from archived Legacy Bureau of Meteorology SST (LBoMSST), $0.01^\circ \times 0.01^\circ$ gridded composite product from 1.1 km High Resolution Picture Transmission (HRPT). LBoMSST stores the most recent high-quality data from a 14 day window; however for this study we have restricted the data to within 5 days. Due to the compilation of multiple satellite sources in the LBoMSST product and limited satellite passes, the oceanographic features are not always displayed exactly at the location of sampling within this image. Depth-integrated major marker pigments for each station (B) expressed in $\mu g/L^{-1}$. Biomarkers are Chl *b*, Divinyl Chl *a* (DV Chl *a*), Zeaxanthin (Zea), Hex-fucoxanthin (19hex), Prasinoxanthin (Prasino), Fucoxanthin (Fuco), But-fucoxanthin (19but), Peridinin. Error bar represent half-interval ($n=2$).

Table 1
Sampling date, location and water mass definition of all stations. Oceanographic features were identified using MODIS and AVHRR satellite data, and confirmed *in situ* using the Bunyip (a highly modified SeaSoar) and the onboard Acoustic Doppler Current Profiler.

Date	Station	Latitude	Longitude	Water mass
11th October 2008	1	−32° 17.99′	155° 21.20′	Oceanic eddy centre
12th October 2008	2	−32° 19.97′	155° 29.02′	Oceanic eddy centre
14th October 2008	3	−32° 30.27′	153° 59.92′	Frontal zone (oceanic eddy-EAC)
15th October 2008	4	−33° 58.47′	152° 24.65′	EAC
15th October 2008	5	−33° 58.15′	151° 60.00′	Coastal eddy centre
15th October 2008	6	−33° 58.14′	151° 40.39′	Inner-shelf
17th October 2008	7	−33° 29.95′	151° 39.84′	Inner-shelf
17th October 2008	8	−33° 30.42′	152° 19.77′	Frontal zone (inner-shelf-EAC)

Nutrient measurements had a standard error $<0.7\%$ and a detection limit of 0.035 μmol L^{-1} for NO_x, 0.012 μmol L^{-1} for Si and 0.009 μmol L_{-1} for PO_4.

To investigate the phytoplankton in different water masses, water was collected at 25, 50, 75 m and the depth of the chlorophyll *a* maximum (Chlmax), as determined by the real-time

Table 2
Dissolved silicate, nitrate and phosphate (μM), total Chl *a* (μg/L^{-1}), maximum quantum yield (Fv/Fm), % of photosynthetic (PSC) and photo-protective (PPC) pigments at the surface (25–30 m), at the depth of the Chl *a* maximum (Chlmax) and depth integrated concentrations (surface to 75 m) at each station. PSC and PPC are given in % of total Chl *a*. Values are given with their standard deviation ($n=3$ for Fv/Fm) and 50% confidence limit ($n=2$) for Chl *a*, PSC and PPC. Nutrient concentration below the analytical detection limit (0.035 μmol L^{-1} for NO_x, and 0.009 μmol L^{-1} for PO_4) is shown as < DL.

Location	Oceanic eddy centre (1)	Oceanic eddy centre (2)	Frontal zone (oceanic eddy-EAC) (3)	EAC (4)	Coastal eddy (5)	Inner-shelf (6)	Inner-Shelf (7)	Frontal zone (inner-shelf-EAC) (8)
Surface temperature (^{o}C)	19.89	18.92	22.36	22.35	19.51	19.63	19.41	20.82
Surface Si (μM)	0.3	0.1	0.1	0.4	0.6	0.4	0.2	0.2
Surface NO_x (μM)	0.1	< DL	< DL	0.3	0.3	1.6	0.3	0.2
Surface PO_4 (μM)	0.1	< DL	< DL	< DL	0.1	0.1	0.1	< DL
Surface Chl a (μg/L^{-1})	0.80 ± 0.03	0.23 ± 0.01	0.12 ± 0.00	0.23 ± 0.00	0.44 ± 0.01	0.51 ± 0.01	0.79 ± 0.03	0.92 ± 0.10
Surface Fv/Fm	0.63 ± 0.02	0.43 ± 0.00	0.62 ± 0.03	0.68 ± 0.00	0.67 ± 0.02	0.65 ± 0.02	0.67 ± 0.02	0.50 ± 0.06
Surface PSC (%)	32 ± 1.5	43 ± 0.2	58 ± 6.4	60 ± 0.2	31 ± 2.3	48 ± 1.3	43 ± 0.9	51 ± 1.4
Surface PPC (%)	19 ± 0.6	34 ± 3.4	33 ± 4.9	46 ± 1.1	10 ± 0.3	12 ± 0.3	10 ± 0.6	12 ± 0.1
Chlmax								
Depth (m)	35	60	70	50	5	50	25	50
Chl *a* (μg/L)	0.61 ± 0.06	0.43 ± 0.01	0.19 ± 0.07	0.48 ± 0.07	0.52 ± 0.02	0.30 ± 0.03	0.90 ± 0.16	1.40 ± 0.08
Chlmax Fv/Fm	0.57 ± 0.00	0.62 ± 0.02	0.63 ± 0.02	0.68 ± 0.2	0.63 ± 0.0	0.67 ± 0.0	0.68 ± 0.0	0.63 ± 0.0
Chlmax PSC (%)	34 ± 0.5	66 ± 0.4	59 ± 2.4	57 ± 2.6	34 ± 0.4	50 ± 2.3	58 ± 0.7	33 ± 1.0
Chlmax PPC (%)	14 ± 0.1	5.8 ± 0.2	17 ± 0.5	17 ± 1.9	12 ± 0.3	6 ± 2.3	6 ± 0.0	9 ± 0.5
Water column integrated								
Chl a (mg/m^2)	37.4	24.5	15.4	21.2	25.2	17.9	67.7	80.1
Si (mmol m^{-2})	50.0	27.0	2.5	45.0	108.8	76.9	123.8	52.5
NO3 (mmol m^{-2})	122.5	57.0	< DL	110.6	281.3	283.1	449.1	140.6
PO4 (mmol m^{-2})	10.0	4.5	< DL	7.5	20.6	18.8	29.1	9.4
Si:N:P	1:2.5:0.2	1:2.1:0.2	1:DL:DL	1:2.5:0.2	1:2.6:0.2	1:3.7:0.2	1:3.6:0.2	1:2.7:0.2

fluorescence profile (Table 2). In addition, water was sampled at stations 1, 3 and 6 to do carbon uptake and nutrient-enrichment experiments (see below). In this case, the water was transferred into 20-30-L LDPE carboys, homogenised and filtered through a 210-μm mesh to remove mesozooplankton grazers. Water was then either sampled for initial parameters (i.e. dissolved nutrients, phytoplankton pigments, photo-physiology) or used in nutrient-enrichment and carbon-uptake experiments.

2.3. Chlorophyll a and accessory pigments

For chlorophyll *a* (Chl *a*) and pigment analyses, 1 L of seawater was gently filtered (max. 5 mm Hg, venturi pump) on a 25-mm GF/F filter (Whatman, glass fibre, 0.7 μm nominal pore size) in duplicate. Each filter was placed in a cryovial and stored in liquid nitrogen (−196 °C) until further analysis. In the laboratory, pigments were extracted at 4 °C in the dark over 15–18 h in 3 mL acetone (100%, diluted to 90% for analysis, Mallinkrodt, HPLC grade) then sonicated on ice for 15 minutes. Samples were recovered using filtration (0.45 μm, Whatman) and centrifugation (2500 rpm, 5 min at 4 °C). The samples were analysed by High Performance Liquid Chromatography (HPLC, Waters—Alliance comprising a 2695XE separations module with column heater and refrigerated autosampler) using a C_8 column (Zorbax Eclipse XDB-C8, Agilent Technologies) and binary gradient system with an elevated column temperature (55 °C) following a modified version of the van Heukelem and Thomas (2001) method. Pigments were identified by their retention time and absorption spectrum from a photo-diode array detector (Waters- Alliance 2996 PDA). Concentrations of pigments were determined from commercial and international standards (Sigma; DHI, Denmark). The HPLC system was also calibrated using phytoplankton reference cultures (Australian National Algae Culture Collection) whose pigment composition has been documented in the literature (Mantoura and Llewellyn, 1983; Barlow et al., 1993; Jeffrey et al., 1997).

Biomarker pigments were used to infer the distribution of dominant algal classes and functional groups. Each biomarker pigment was normalised against total Chl *a* to account for spatial variation of the total algal biomass. In this work, total Chl *a* is abbreviated as Chl *a* and equals the sum of monovinyl (MV) and divinyl (DV) Chl *a*. Briefly, biomarkers represent the following phytoplankton classes: Chlorophytes (Chlorophyll *b*, [Chl *b*] and Lutein, [Lut]), Cyanobacteria (Zeaxanthin, [Zea]), Cryptophytes (Alloxanthin, [Allo]), Prymnesiophytes (19'Hexanoyloxyfucoxanthin, [19 Hex]), Pelagophytes (19'Butanoloxylfucoxanthin, [19But]), Prasinophytes (Prasinoxanthin, [Prasino]), Diatoms, Prymnesiophytes, Chrysophytes Pelagophytes and Raphidophytes (Fucoxanthin, [Fuco]), and autotrophic dinoflagellates (Peridinin, [Per]). More details can be found in Jeffrey et al. (1997). The photosynthetic (PSC) and photo-protective (PPC) pigment contributions were calculated as per Barlow et al. (2007). Briefly, PSC is the sum of Per, 19Hex, 19But and Fuco and PPC is the sum of diadinoxanthin (Diadino), Allo, diatoxanthin (Diato), Zea, Violaxanthin (Viola) and carotenes. Here, PSC and PPC are expressed in percentage, relative to total Chl *a*.

2.4. Photo-physiological parameters

The activity of photosystem II (PSII) in phytoplankton was studied using a WaterPAM (Heinz Walz GmBH, Effeltrich, Germany) and WinControl software (version 4.06). The level of fluorescence emitted by the sample (3 mL in a quartz cuvette) was measured under a weak measuring light (0.15 μmol photon m^{-2} s^{-1}) that induced fluorescence emission (F' or F_0 depending on dark adaptation) without causing any electron transport. The maximum level of fluorescence (Fm) was then recorded during a short (0.6 s) saturating light pulse (10,000 μmol photon m^{-2} s^{-1}). Effective quantum yield (Φ) was measured shortly after sample collection whereas the maximum quantum yield (Fv/Fm) was measured following a 5 min dark adaptation period to ensure that no electrons remained in the electron transport chain and Chl *a* was unexcited. During the saturating light pulse, all reaction centres capture electrons and remain closed until transfer along the electron transport chain. The maximum quantum yield, related to the number of reaction centres participating in the light capture, is given by:

$$F_v/F_m = (F_m - F_0)/F_m \quad (1)$$

2.5. Nutrient-enrichment experiments

The phytoplankton response to nutrient enrichment was investigated at Stations 1, 3 and 6, representing the centre of the oceanic eddy, the frontal zone between the eddy and EAC, and inner-shelf water, respectively. A constant depth (25 m), rather than the depth of Chlmax, was chosen to avoid phytoplankton variability due to differences in light acclimation. The following nutrient enrichments were added to duplicate 2 L polycarbonate bottles at $t=0$ and every subsequent 24 h:

1. No addition (Control, C)
2. + NO_3 (10 μM)
3. + NH_4 (10 μM)
4. + NO_3(10 μM)+Si(10 μM)+PO_4(0.6 μM)=Mix
5. + Si (10 μM)

The level of nutrient enrichment was chosen by considering nutrient concentrations in NSW coastal waters and the biological requirement of key phytoplankton functional groups (e.g., diatoms, cyanophytes, prochlorophytes and prymnesiophytes, Sarthou et al., 2005; Schoemann et al., 2005; Veldhuis et al., 2005). The Mix enrichment was conducted in Redfield (1958) proportions. Incubation water was sub-sampled at 0, 24 and 48 h for effective quantum yield. Bottles were incubated at ambient sea-surface temperature in an on-deck incubator covered with blue-mesh screening to reduce incident light by 75%. Light intensity and temperature were recorded *in situ* in real-time using data loggers (HOBO Pendant, Onset, USA) during the three experiments. The average light level in the incubators across all three experiments was ~70 μmol photon m^{-2} s^{-1} and temperature was 21 °C. After 65–68 h, sub-samples were collected for estimates of carbon uptake (detailed below). Nutrients were measured following the first nutrient enrichment (t=initial) and at the end of the incubation. Initial and final concentrations of total Chl *a* were used to calculate a daily growth rate in each experimental treatment as:

$$\mu(\mathrm{day}^{-1}) = \frac{\ln Chl\,a_{\mathrm{final}} - \ln Chl\,a_{\mathrm{initial}}}{\Delta \mathrm{days}} \quad (2)$$

2.6. Carbon-uptake experiments

In conjunction with nutrient-enrichment experiments, carbon uptake of phytoplankton was investigated. Water (25 m depth) from Stn 1, 3 and 6 was dispensed into nine 200-mL polycarbonate bottles, stored for one hour in the dark then spiked with $NaH^{14}CO_3$ (Perkin Elmer, at specific activity of 0.25 μCi/mL). Each bottle was sampled for initial ^{14}C analysis (0.5 mL) prior to

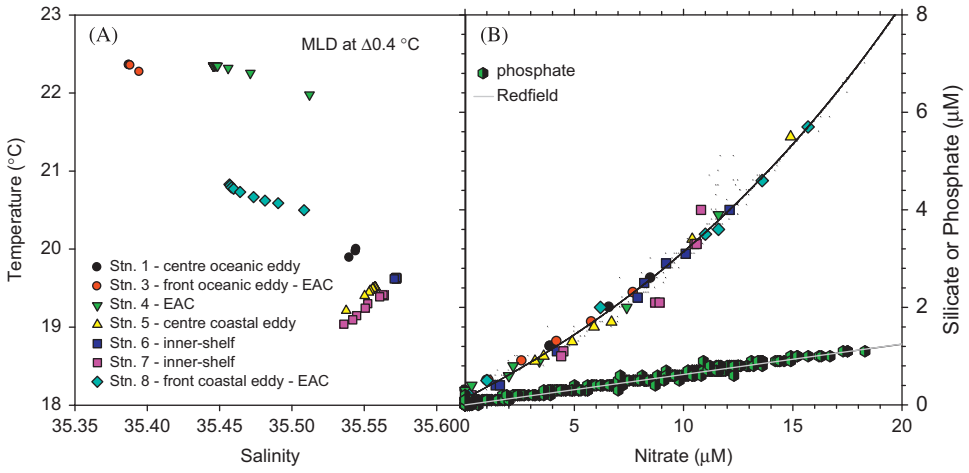

Fig. 2. Temperature–Salinity profiles of the mixed layer at different stations (A). The depth of the mixed layer was calculated considering a maximal difference of 0.4 °C with surface water. Depth of the mixed layer was much shallower for stations 1 and 3 (8 and 14 m, respectively) than the other stations (30–38 m for Stns. 4–7; 22 m for Stn 8). Representation of dissolved NO_3, Si and PO_4 concentrations for all stations 1 to 8 (B). The ratio NO_3:PO_4 (dual colour circles) is shown with the Redfield ratio (16:1, thick grey lines). NO_3 to Si ratio within the mixed layer at all stations is shown as in panel A. The consumption of NO_3 and Si was fitted using an exponential growth model (Stirling Model, curved line) $y=y_0+a^*(\exp(b^*x)-1)/b$ where $x=[NO_3]$ and $y=[PO_4]$, $y_0=0.13$, $a=0.23$ $b=0.052$.

being incubated for 2–3 h at ambient sea-surface temperature in an incubator under various light levels (Dark (double wrapped with aluminium foil), 50, 95, 165, 235, 300, 365, 450, and 570 μmol photon m^{-2} s^{-1}). In addition to incubation at different light levels, carbon uptake was also measured at an intermediate light level (235 μmol photon m^{-2} s^{-1}, close to half-saturating level) following incubation (65–68 h) for all nutrient enrichments. Following incubation, bottles were stored in the dark (to stop ^{14}C fixation) until contents was filtered on GF/F filters (0.7 μm pore size, 13 mm, Whatman) under low vacuum (<5 mm Hg). Filters were rinsed using filtered seawater to remove any ^{14}C not associated with the biota and then placed on absorbent paper in a dessicator with NaOH pellets in a fume hood. To induce the degassing of non-fixed ^{14}C (e.g. adsorbed on the outside of the biota), 30 μL of HCl 0.1 M was dispensed on each filter and left to react for at least 1 h. The filters were then placed into scintillation vials and 100–200 μL NaOH 0.1 M plus 10 mL of scintillation cocktail (Ultima Gold, Perkin Elmer) were added. Under these conditions, the pH was >9 which prevented further loss of ^{14}C.

Back in the laboratory, scintillation vials were vortexed and the amount of ^{14}C was measured (counts per minute, CPM) using a liquid scintillation β-counter (Wallac 1409). CPM were converted into disintegrations per minute (DPM) using a built-in quench curve for ^{14}C. DPM were transformed into a value representing the concentration of fixed carbon (μmol L^{-1} or μg L^{-1}) considering a dissolved inorganic carbon concentration of 2050 μmol L^{-1}, the specific activity of the source used, duration and volume of incubation as per Hassler and Schoemann (2009).

Non-linear curve fitting of the carbon fixed at different light levels was used to estimate the saturating light level and the maximum carbon uptake of the phytoplankton community. Due to a minimal ^{14}C uptake in the dark, our analysis was limited to a simple non-linear curve fitting (4 parameters logistic curves, Sigma Plot, ver. 10) rather than using the hyperbolic curve fit as per Jassby and Platt (1976). Non-linear fittings of the data were satisfactory with $r^2 > 0.94$ (18 points), with 95% confidence intervals for half-saturation light representing 4 to 13% of its value.

2.7. General precautions and statistical tests

As a general precaution to avoid nutrient as well as biological cross-contamination, all containers were rinsed three times with MilliQ ultrapure water prior to being used. In addition, for on-deck incubations, the same bottles were reused for identical experimental treatments.

Analysis of HPLC pigment data was performed using Primer (ver. 6.1). Data from each station was transformed with a 4th root transformation and a matrix of similarity (resemblance) generated. Multi-dimensional scaling (MDS) was then applied to determine similarities between water masses. An analysis of similarities (ANOSIM) was then used to determine which pigments had the greatest contribution to distinguishing the different water masses. Differences in phytoplankton biomass in nutrient-enrichment treatments were assessed using a Student t-test at a 95% confidence level.

3. Results

3.1. Physical characterisation of water masses

Sea-surface temperatures in the study region were dynamic, as shown by the composite plot in Fig. 1(A), where water masses were moving too quickly for a single satellite image to accurately reflect conditions on different sampling dates. Vertical temperature–salinity profiles however, clearly distinguished different water masses (Fig. 2 A). Water in the surface mixed layer was relatively warm in the EAC (Stn 4, 22.4 °C) and at the offshore frontal zone where the EAC and oceanic cold-core eddy converged (Stn 3, >22 °C, Fig. 2 A). Water at the centre of the oceanic eddy (Stn 1) and on the inner-shelf (Stns 5, 6 and 7) was colder (<19.5 °C). Interestingly, water in the frontal zone between the EAC and inner-shelf water (Stn 8) had intermediate salinity and temperature as compared to the other stations. The contour plots representing the transects show that both the offshore oceanic eddy and the inner-shelf eddy had decreased temperature at the centre and doming of the isotherms (Figs. 3A and 4A), typical of cold-core eddies (Mann and Lazier, 2006). The doming of the isotherms is more apparent in the coastal eddy (Fig. 4A) than in the oceanic eddy (Fig. 3A).

3.2. Water masses and nutrient distributions

There were strong horizontal and vertical gradients in dissolved nutrients across the study region. As expected, nutrient

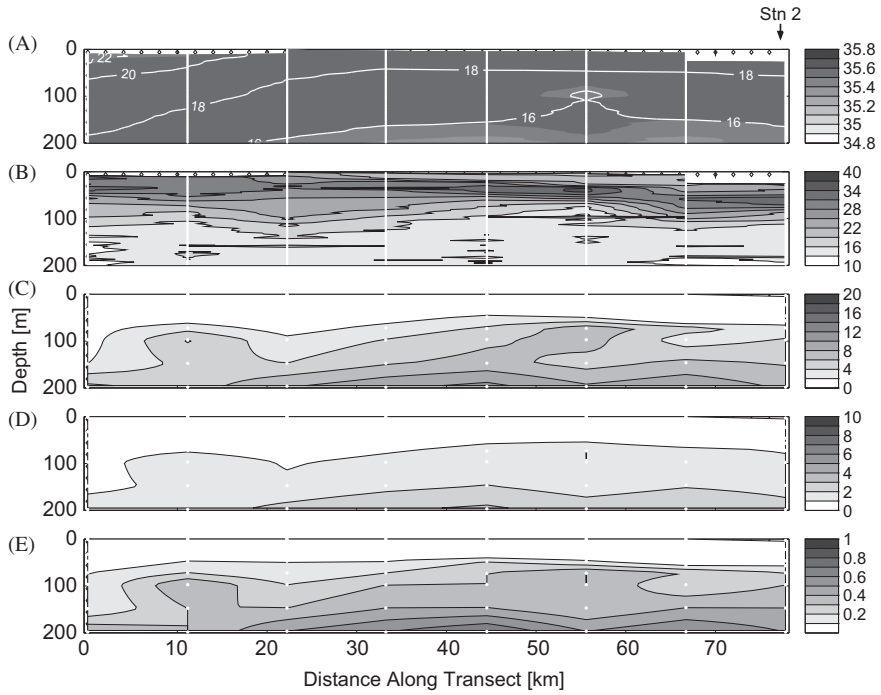

Fig. 3. CTD transect from the edge of the offshore eddy (EAC) to the centre. Panels show (A) Temperature/Salinity, (B) Fluorescence, (C) Nitrate, (D) Silicate and (E) Phosphate. The thin white lines indicate the electronic CTD casts with measurements taken each metre. The nitrate, phosphate and silicate concentrations are obtained from bottle samples from the location indicated by a white dot. The transect was undertaken in a southward direction from 02:15 to 14:10 on 12 October 2008 (Australian Eastern Daylight-Saving Time).

concentrations were higher on the inner-shelf compared to the EAC (Stn 4; Figs. 3 and 4 panels C, D and E). Furthermore, nitrate, silicate and phosphate distributions showed relatively consistent depletion across the oceanic cold-core eddy down to at least 50 m (Fig. 3C, D, E). Subsurface nutrient concentrations were elevated near the centre of both eddies (Stns 2 and 5), however nutrient concentrations were significantly higher in the coastal eddy (Figs. 2 and 3, Table 2). Dissolved nutrient concentrations were also depleted in the surface (down to approximately 30 m) of the coastal eddy but tended to decrease across the shelf with increasing distance from the coast (Fig. 4 C, D, E). The onshore side of the coastal eddy (Stn 6) showed nutrient enrichment relative to the EAC edge (i.e. offshore) of the eddy (Stn 4). Interestingly, the coastal transect spanning stations 7 and 8 had higher dissolved nutrients than the more southerly transect across the coastal eddy, with silicate being relatively more depleted than nitrate (Fig. 5 C and D).

3.3. Chl *a* fluorescence and phytoplankton biomass

Chl *a* fluorescence varied between water masses, being greatest in the coastal eddy (Stn 5) and inner-shelf-EAC frontal zone (Stn 8) compared to the EAC (Stn 4) and oceanic eddy (Stn 2; Figs. 3–5 panel B). Vertical profiles showed sub-surface Chl *a* fluorescence maxima between 5 and 100 m, confirmed by pigment extraction and subsequent HPLC analyses. The depth of the maximal Chl *a* (Chlmax) at the centre of the oceanic and coastal eddies was at 35 and 5 m, respectively, as compared with 60–70 m at the frontal zone between the oceanic eddy and the EAC and 50 m in inner-shelf waters (Table 2). As expected from the MODIS satellite images, phytoplankton biomass at a depth of 25 m was highest in inner-shelf waters and in the frontal zone between the inner-shelf and the EAC, but was also relatively high in the centre of the oceanic eddy when it was first sampled (Stn 1; Table 2). Water-column-integrated Chl *a* was 3–4 times greater in the inner-shelf-EAC frontal zone and adjacent inner-shelf waters (Stns 8 and 7, respectively) compared to the EAC and frontal zone between the EAC and oceanic eddy (Stns 4 and 3, respectively; Table 2), with intermediate values in the centre of the oceanic and coastal eddies (Stns 1, 2, 5; Table 2).

3.4. HPLC biomarker pigments

There was little change in the proportion of photosynthetic pigments (PSC) with depth, except at the frontal zone of the oceanic eddy (Stn 3), where they increased 26% between 25 and 60 m (data not shown). Lowest proportions of PSC (31–32%) at a depth of 25 m were observed in the centre of the eddies (Stns 1 and 5) whereas greater PSC was observed in the EAC (Stn 4) and the frontal zone where the EAC converged with the oceanic eddy (Stn 3; Table 2). In contrast, the proportion of photo-protective pigments (PPC) was consistently greater at the surface compared to deeper stations across all water masses (data not shown). At 25 m depth, there was a 2–4-times greater PPC percentage in the EAC (Stn 4) and at oceanic eddy stations (Stns 2 and 3) as compared to the other stations (Table 2).

Biomarker pigments demonstrated contrasting phytoplankton communities in the different water masses (Fig. 1B, 6). DV Chl *a* and DV Chl *b*, biomarkers for prochlorophytes, typical of tropical phytoplankton communities (Goericke and Repeta, 1992) were only detected in the EAC (Stn 4). Chlorophytes (Chl *b* and zeaxanthin) and cyanophytes (zeaxanthin alone) were only found within the oceanic eddy (Stns 1–3) and the EAC (Stn 4). Chlorophytes (Chl *b* in absence of zeaxanthin) were found in all inner-shelf surface waters (25 m), including the coastal eddy (Stns 5–8; Fig. 1 B, 6). The greatest concentration of peridinin (a biomarker for dinoflagellates) was detected in the inner-shelf-EAC frontal zone and in the coastal eddy (Stns 5 and 8; Fig. 1 B, 6).

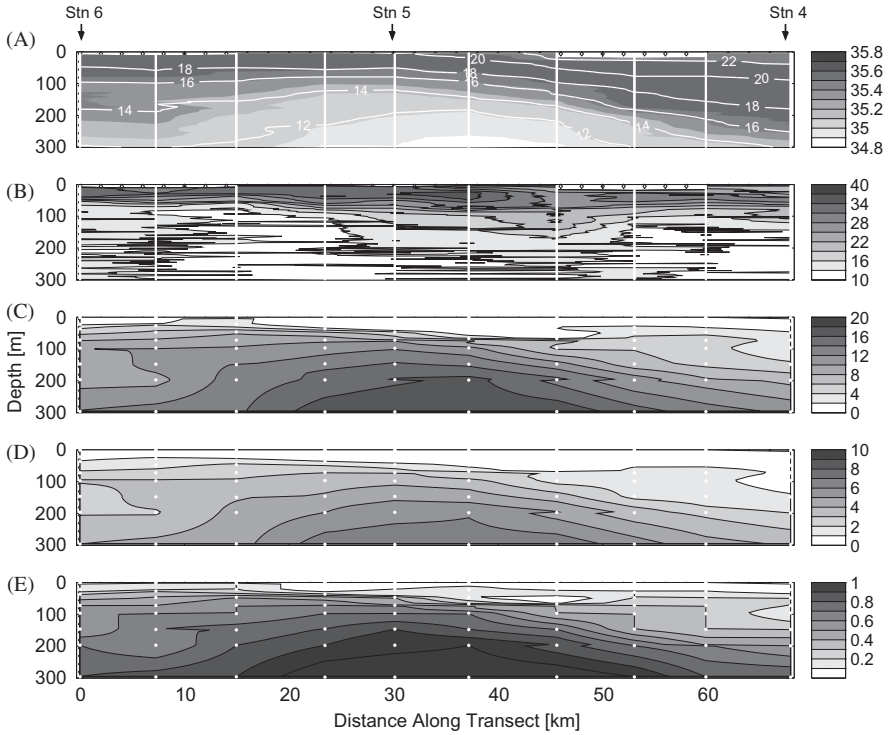

Fig. 4. CTD transect from the coastal waters off Sydney, through a coastal cold-core eddy to the East Australian Current. Panels show (A) Temperature/Salinity, (B) Fluorescence, (C) Nitrate, (D) Silicate and (E) Phosphate. The thin white lines indicate the electronic CTD casts with measurements taken each metre. The nitrate, phosphate and silicate concentrations are obtained from bottle samples from the location indicated by a white dot. The transect was undertaken in an easterly direction from 10:00 to 23:50 on the 15th October 2008 (Australian Eastern Daylight-Saving Time).

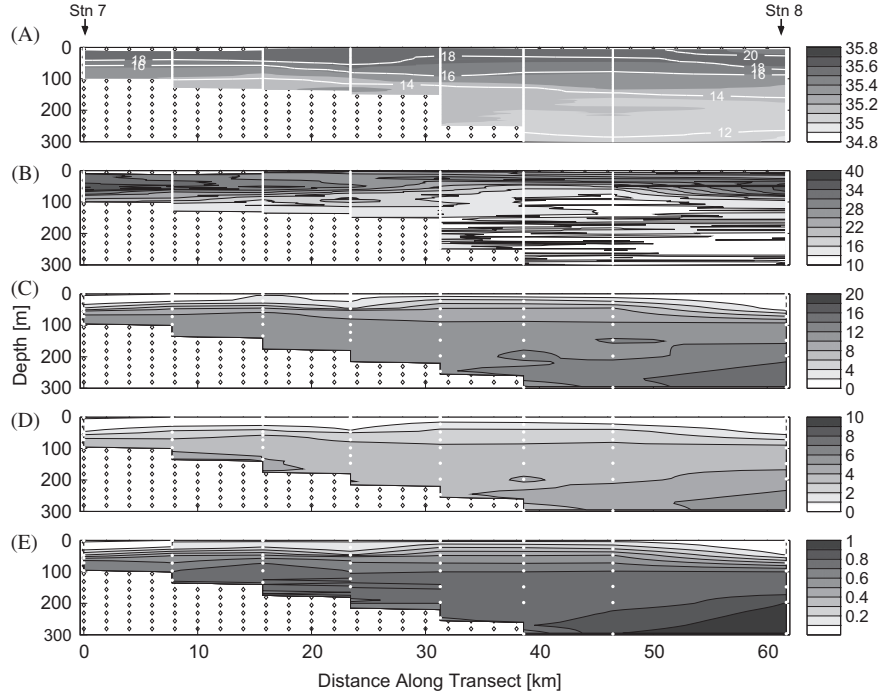

Fig. 5. CTD transect of the coastal waters off Broken Bay. Panels show (A) Temperature/Salinity, (B) Fluorescence, (C) Nitrate, (D) Silicate and (E) Phosphate. The thin white lines indicate the electronic CTD casts with measurements taken each metre. The nitrate, phosphate and silicate concentrations are obtained from bottle samples from the location indicated by a white dot. The transect was undertaken in an easterly direction from 04:30 to 13:45 on the 17th October 2008 (Australian Eastern Daylight-Saving Time).

This biomarker was also present in surface waters (25 m) of inner-shelf waters (Stns 6 and 7) and inside the oceanic eddy (Stn 1). In fact, in inner-shelf waters and in the coastal eddy (25 m depth, Stns 5–8), phytoplankton communities were similar, dominated by chlorophytes (Chl *b*) and diatoms (Stns 6–8) with minor presence of prasinophytes and dinoflagellates. It is only in the

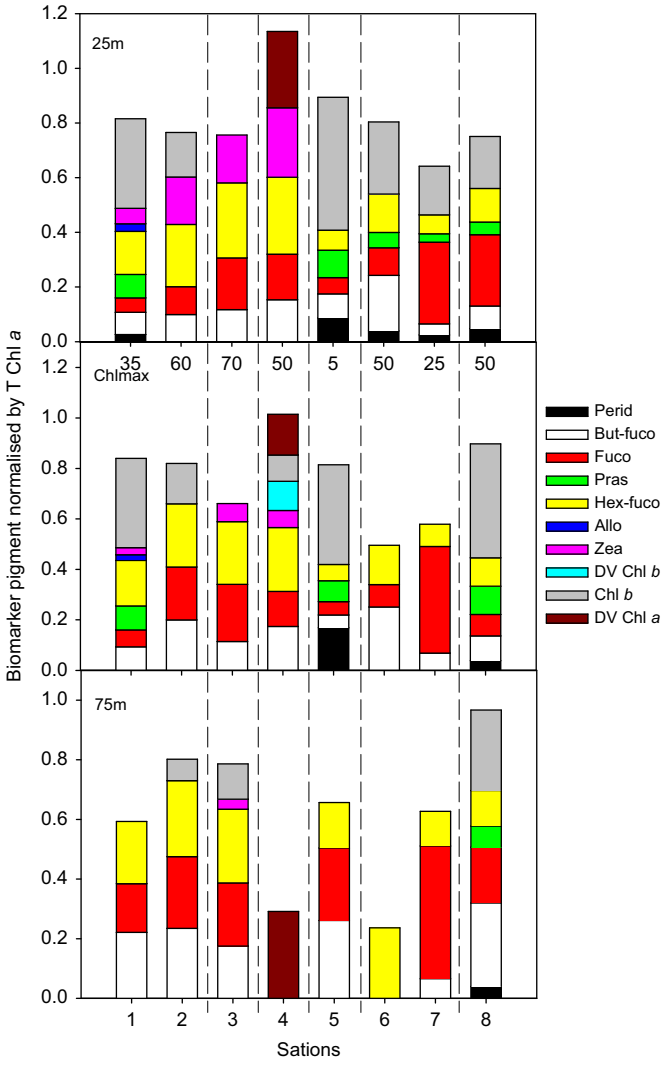

Fig. 6. Biomarker pigments of dominant algal classes normalised by total Chl *a* (average value, $n=2$) are given at depth of 25 m, Chlmax (depth indicated on the top of each vertical bar) and 75 m for all Stns. Stns are presented according to water mass: (A) inside the oceanic cold-core eddy, (B) frontal zone oceanic eddy and East Australian Current (EAC), (C) East Australian Current, (D) inner-shelf water, and (E) coastal eddy and frontal zone between inner-shelf and the EAC. Oceanographic features were identified using MODIS image and BlueLink output. Biomarkers are Divinyl Chl *a* (DV Chl *a*), Chl *b*, Divinyl Chl *b* (DV Chl *b*), Zeaxanthin (Zea), Alloxanthin (Allo), Hex-fucoxanthin (Hex-fuco), Prasinoxanthin (Pras), Fucoxanthin (Fuco), But-fucoxanthin (But-fuco), Peridinin (Perid).

frontal zone between inner-shelf waters and the EAC (Stn 8), that biomarkers for chlorophytes and dinoflagellates were detected below a depth of 25 m. At all other inner-shelf stations (Stns 5, 6 and 7), the phytoplankton community was dominated by diatoms and pelagophytes at depth (Fig. 6). Fucoxanthin concentrations were greatest in the inner-shelf waters, being an order of magnitude greater in the frontal zone with the EAC (25 m) and at the Chlmax at Stn 7 than for other inner-shelf waters (Fig. 6). Similarly, diadinoxanthin was significantly greater in the centre of the coastal eddy and inner-shelf waters compared to other water masses (data not shown), indicating a greater abundance of diatoms, chrysophytes and prymnesiophytes (Kruskal–Wallis, Chi-square=12.6, df=5, $p=0.03$). Although biomarkers (Fig. 6) indicate that diatoms were present at some stations in inner-shelf waters, diatoms only dominated the phytoplankton community at station 7 and possibly station 8 (25 m only). Other major groups of phytoplankton were chlorophytes, prymnesiophytes, pelagophytes, cyanophytes and prochlorophytes (Fig. 6).

At depths of 25 m and Chlmax, the phytoplankton community in the EAC (Stn 4) was similar to the community observed at the frontal zone of the oceanic eddy and the EAC (Stn 3; Fig. 6). The phytoplankton community at the centre of the oceanic eddy (Stn 1) more resembled the phytoplankton community in inner-shelf waters, especially the community found in the coastal eddy (Stn 5,

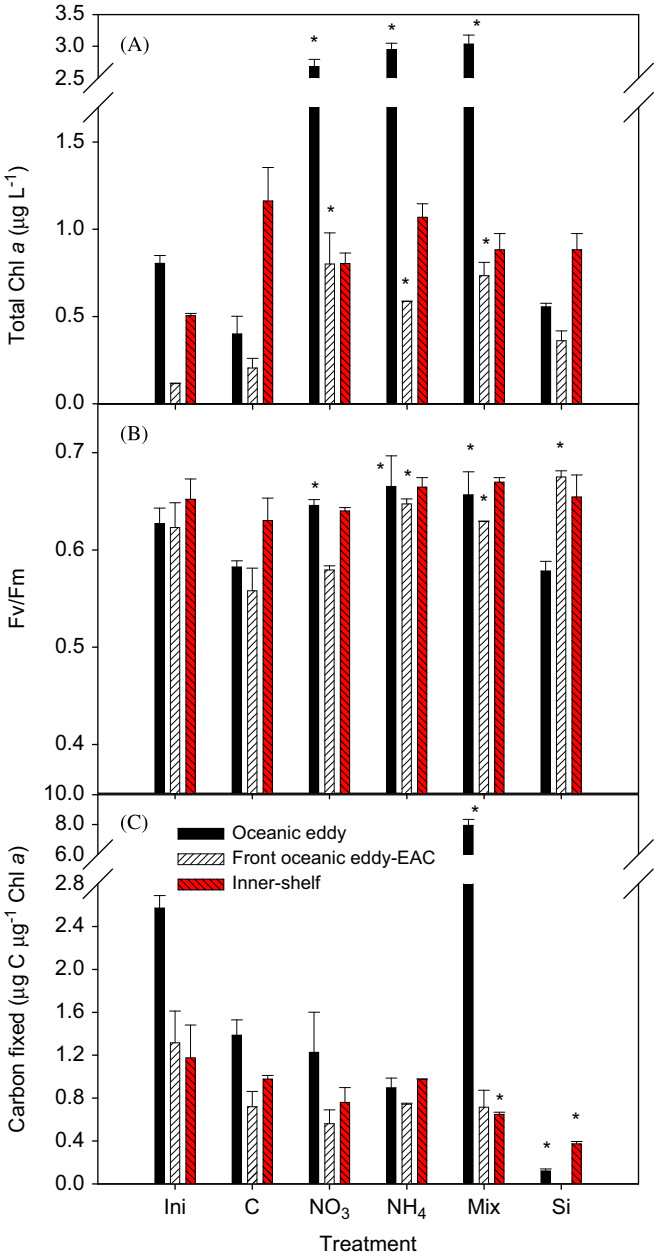

Fig. 7. Total Chl *a* (A), maximum quantum yield (Fv/Fm; B) and carbon fixation (C) of phytoplankton before (Ini) and after nutrient enrichment. Samples were collected at 25 m in different water masses in the separation zone of the East Australian Current: in the centre and at the frontal zone between an oceanic cold-core eddy and the EAC, and in inner-shelf water near Sydney. Duplicate samples were incubated at sea-surface temperature with a daily average light intensity of 70 µmol photon m^{-2} s^{-1} with daily addition of nutrients as follows: none (control, C), NO_3 (10 µM), NH_4 (10 µM), Mix (NO_3:PO_4:Si , 10:0.6:10 µM), and Si (10 µM). Error bars represent the half interval ($n=2$, total Chl *a* and carbon fixation) and the standard deviation ($n=4$–6, Fv/Fm) associated with the average values. Statistical differences (t-test at level 0.05) between the control and any nutrient enrichment are indicated by an asterisk.

Fig. 6). Although both stations 1 and 2 were in the oceanic eddy, the biomarker pigments showed significant differences (Fig. 6).

Using pigments normalised to Chl *a* biomass, the multivariate analysis revealed large differences in phytoplankton communities across some water masses (46–90% similarity between surface communities; 52–92% similarity at the Chl-*a* maximum; and 67–86% similarity across the upper 95 m). Phytoplankton communities in the frontal zones either side of the EAC were the most different (i.e. only 50–67% similarity, Stns 3 and 8) from other water masses. This outcome was consistent across surface, Chlmax or data from all depths. The EAC community was distinct from the inner-shelf-EAC frontal zone and inner-shelf communities (64–75% similarity). The phytoplankton community in the centre of the coastal eddy also showed relatively large differences with adjacent water masses, particularly at the surface (only 66–75% similarity between the eddy centre and the EAC and EAC frontal zone), but was similar to the pigment composition at the centre of the oceanic cold-core eddy (85% similar). Interestingly, the surface phytoplankton communities generally contrasted more strongly than those at the Chlmax or across all depths in the upper 95 m.

3.5. Photo-physiology and carbon uptake

High maximum quantum yields (Fv/Fm, >0.6; Table 2) were measured at most stations. A Fv/Fm lower than 0.50, often associated with stressed phytoplankton communities, was only measured in surface water (25 m) at station 2 in the oceanic eddy (Fv/Fm=0.43, Table 2).

With respect to carbon uptake, phytoplankton communities in the centre of the oceanic eddy (Stn 1) and the frontal zone between the oceanic eddy and the EAC (Stn 3) had similar saturating and half-saturating light levels of 494 ± 74 and 248 ± 16 μmol photon m^{-2} s^{-1} inside the eddy; 504 ± 71 and 297 ± 16 μmol photon m^{-2} s^{-1} in the frontal zone. Phytoplankton at station 6 (inner-shelf) had a slightly lower saturating light level (415 ± 19 μmol photon m^{-2} s^{-1}), but similar half-saturating light level (272 ± 5 μmol photon m^{-2} s^{-1}). Maximum carbon fixation rates in the oceanic eddy (5.9 ± 0.8 gC gChl a^{-1} L^{-1} h^{-1}) and at the frontal zone between the oceanic eddy and EAC (6.0 ± 0.5 gC gChl a^{-1} L^{-1} h^{-1}) were higher than in inner-shelf water (4.8 ± 0.2 gC gChl a^{-1} L^{-1} h^{-1}).

The carbon fixed by the phytoplankton community present inside the oceanic eddy (Stn 1; 49.7 ± 3.2 μg C d^{-1}) was 13 and 3 times higher than the phytoplankton community at the frontal zone of the oceanic eddy and the EAC (Stn 3; 3.7 ± 1.2 μg C d^{-1}) and in inner-shelf water (Stn 6; 14.5 ± 5.3 μg C d^{-1}), respectively. Interestingly, the rate of carbon fixation per unit of biomass measured at 235 μmol photon m^{-2} s^{-1} was 2 times greater inside the oceanic eddy (Stn 1) as compared to the frontal zone of the oceanic eddy and the EAC (Stn 3) and inner-shelf water (Stn 6; Fig. 7 C, initials).

3.6. Nutrient limitation of phytoplankton growth

Dissolved nutrient concentrations and phytoplankton biomass (total Chl *a*) were appreciably different for the three stations where nutrient-enrichment assays were performed. The initial nutrient concentrations were greatest in inner-shelf water (Stn 6) and lowest at the oceanic eddy-EAC frontal zone (Stn 3), with intermediate concentrations in the centre of the oceanic eddy (Stn 1; Table 2). The total Chl *a* concentration in surface water was 7 fold greater inside the oceanic cold-core eddy compared to the frontal zone (Table 2, Fig. 7A initials). The phytoplankton communities at stations 1, 3 and 6 were also very different (Fig. 6). Briefly, inside the oceanic eddy, the dominant pigments were MV Chl *b*, hex-fucoxanthin, and prasinoxanthin, suggesting a community of prochlorophytes, prymnesiophytes and prasinophytes. At the eddy-EAC frontal zone, the dominant pigments were hex-fucoxanthin, fucoxanthin, and but-fucoxanthin, suggesting a community dominated by prymnesiophytes, pelagophytes and possibly diatoms. At the inner-shelf station, the dominance of but-fucoxanthin and diadinoxanthin suggested the presence of diatoms and pelagophytes.

Following nitrogen enrichment of oceanic eddy water (i.e., NO_3, NH_4 and NO_3:PO_4:Si (Mix) addition), there was a significant increase (6–7-fold) in total Chl *a* (Student t-test, $p<0.05$) compared to the control (Fig. 7A). This suggests that the phytoplankton community in the centre of the oceanic eddy was nitrogen limited. Total Chl *a* decreased in both control and Si treatments, suggesting exhaustion of the limiting nutrient during incubation. During the incubation, the concentration of dissolved NO_x decreased from 0.12 μM to below detection in both the control and Si treatment. Phytoplankton only showed a positive

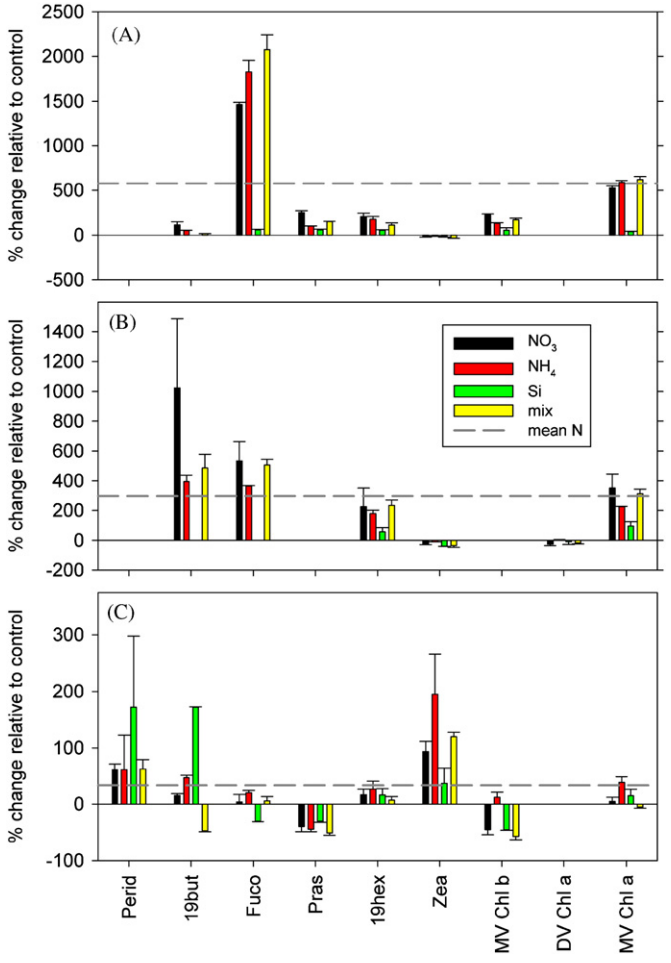

Fig. 8. Mean major biomarker pigments ~3 days after nutrient enrichment normalised to the control treatment (no added nutrients). Samples were collected at the depth of 25 m in contrasting regions in the separation zone of the East Australian Current: inside an oceanic eddy (A), at the frontal zone between the oceanic eddy and the EAC (B) and in inner-shelf water off Sydney (C). Duplicate samples incubated at sea-surface temperature with a daily average light intensity of 70 μmol photon m^{-2} s^{-1} and a daily addition of nutrients as follows: none (control, C), NO_3 (10 μM), NH_4 (10 μM), Mix (NO_3:PO_4:Si , 10:0.6:10 μM), and Si (10 μM). Biomarker pigments divinyl Chl *a* (DV Chl *a*), monovinyl Chl *b* (MV Chl *b*), zeaxanthin (Zea), 19′-hexanoyloxyfucoxanthin (19hex), prasinoxanthin (Pras), fucoxanthin (Fuco), 19'butanoyloxyfucoxanthin (19but), peridinin (Perid) are shown. Error bars represent half interval ($n=2$). The dotted line is the average increase in MV Chl *a* in the three treatments with added nitrogen (NO_3, NH_4, Mix) relative to control. Marker pigments above the dotted line increased faster than the overall community (MV Chl *a*) while those below increased more slowly.

growth rate in NO_3 ($0.40 \pm 0.02\ d^{-1}$), NH_4 ($0.43 \pm 0.02\ d^{-1}$) and Mix ($0.45 \pm 0.03\ d^{-1}$) enrichments with the average MV Chl *a* concentration increasing ~580% relative to the control.

At the frontal zone between the oceanic eddy and EAC (Stn 3), all nitrogen enrichments (i.e. NO_3, NH_4 and Mix treatments) induced an average MV Chl *a* increase of ~300%, somewhat less than Stn 1 (Fig. 7A). At Stn 3, dissolved NO_x concentrations were below the detection limit. Following incubation, there was a 4-fold decrease in dissolved Si and 2-fold decrease in dissolved PO_4 concentrations in the control with growth occurring in all treatments. Growth rates were greater than at Stn 1 in the NO_3 ($0.69 \pm 0.08\ d^{-1}$), NH_4 ($0.59 \pm 0.01\ d^{-1}$) and Mix ($0.67 \pm 0.03\ d^{-1}$) treatments. A high growth rate was also measured for the Si enrichment ($0.41 \pm 0.06\ d^{-1}$) as compared to the control treatment ($0.20 \pm 0.11\ d^{-1}$).

In contrast to Stns 1 and 3, there was a very limited response to any nutrient enrichment in the inner-shelf water (Stn 6, Fig. 7). A positive growth rate ranging from 0.13 to $0.29\ d^{-1}$ was found in all treatments with the highest growth rate in the control. Nutrient consumption was detected in the control treatment (1.4–3.0-times decrease) but considerable concentrations were still available in the control bottles at the end of the experiment; Si, PO_4 and NO_x in the control bottles were 0.29, 0.05 and 0.56 μM, respectively. These concentrations were greater than those initially measured at Stns 1 and 3 (Table 2).

There was a decrease in Fv/Fm in control bottles (control) in the centre of the oceanic eddy and at the frontal zone (Fig. 7 B), suggesting that the health of the community was decreased, probably resulting from nutrient depletion. Inside the oceanic eddy, similar to observations of total Chl *a* (Fig. 7A), a significant increase in Fv/Fm was measured under all nitrogen enrichments (Fig. 7B). At the frontal zone between the oceanic eddy and the EAC (Stn 3), a significant increase of Fv/Fm was measured for all nutrient enrichments except NO_3. No significant changes in Fv/Fm were observed in coastal waters. For treatments that were statistically higher than the control, an increase in effective quantum yield well as an increased in the level of total fluorescence was recorded after 24 h incubation (data not shown).

Nutrient enrichment caused a 7 and 4-fold increase in the total carbon fixed inside the oceanic eddy and at the oceanic eddy-EAC frontal zone, respectively (data not shown). Given that nutrient enrichments induced a community shift in the dominant group of phytoplankton (see below, Fig. 8), the capacity to fix carbon was normalised per unit of biomass (i.e. total Chl *a*, Fig. 7C) for comparison. In the absence of nutrient enrichment (control), the rate of carbon fixation per unit of biomass decreased for the three stations, with the greatest decrease inside the oceanic eddy. In most cases, there was no difference in carbon fixed per unit of biomass in nutrient enriched treatments compared to the control (Fig. 7C). A marked increase in carbon fixation per unit of biomass was only observed for the Mix treatment at Stn 1. A significant decrease in carbon fixation per unit of biomass was observed for the Si treatment at Stns 1 and 3 and for the Mix treatment at Stn 3.

Based on biomarkers (Fig. 8A), a shift in the phytoplankton community followed all nitrogen treatments inside the oceanic eddy (Stn 1), resulting in a relative decrease in all marker pigments except fucoxanthin. The increase of fucoxanthin relative to MV Chl *a* indicated that only diatoms were able to exploit the added nitrogen. Compared with the control treatment, all nitrogen enrichments showed a decrease in the relative importance of chorophytes (Chl *b* and zeaxanthin), prymnesiophytes, prasinophytes, protochlorophytes and cyanophytes. At this station NO_3, NH_4 and Mix treatments showed low pigment dissimilarity (4–6%), and highest percentage of dissimilarity between control and NH_4 (27%). The community selected following all nitrogen enrichment had very low dissimilarities with inner-shelf waters from station 7.

A shift in the phytoplankton community in response to nutrients (N and Si) was also observed at the frontal zone oceanic eddy-EAC (Stn 3; Fig. 8B). Following any enrichment, the abundance of zeaxanthin was decreased whereas Chl *b* remained constant. This suggests a decrease in cyanophytes or prochlorophytes whereas prymnesiophytes (hex-fucoxanthin), pelagophytes (but-fucoxanthin) or diatoms (fucoxanthin) increased in response to nutrient enrichment. For water collected at Stn 3, the greatest similarity was observed between NH_4 and Mix treatments (4.5% dissimilarity) followed by NH_4 and Si vs. NO_3 (9%). The greatest dissimilarity was observed between NH_4 and Mix treatments vs. initial (34%).

Despite nutrient enrichment of inner-shelf water (Stn 6), there were no significant differences in total Chl *a*, and Fv/Fm (Fig. 7), biomarker pigments at the end of incubations (Fig. 8C) show small differences between treatments, suggesting that the composition of the phytoplankton community was affected (Fig. 8C). It is to be noted that the magnitude of change in biomarker pigments is much smaller than for Stns 1 and 3 (see scale of *y*-axis in Fig. 8). Dinoflagellates and cyanophytes slightly increased while prasinophytes and chlorophytes decreased. In this case, the composition of the phytoplankton community was not strongly affected by any of the experimental treatments and had lowest dissimilarity between treatments (5–11%).

4. Discussion

4.1. Spatial and temporal variability

This study highlights the physical, chemical and biological heterogeneity of the separation zone of the EAC resulting in complex biological gradients along both the north–south and east–west axes with eddies adding another level of complexity. Previous studies have demonstrated heterogeneous water masses in this area (e.g., Tranter et al., 1986; Cresswell, 1994; Oke and Middleton, 2001; references therein). In this region, both spatial and temporal variability can be high and water mixing, source and time since upwelling, nutrient supply rate and rate of biological consumption will all be important in defining the phytoplankton community present. For example, during October 2008 the northeast sector of this study region was nutrient deplete with a relatively mature phytoplankton community while the southwest was still nutrient replete. The oceanic eddy sampled in the northeast sector was approximately 2 months old with depleted surface nutrients as a result of biological activity, while the coastal eddy was formed only days prior to sampling. In the oceanic eddy, based on fluorescence profiles, algal biomass was greater than in surrounding waters, as opposed to what is observed in the coastal eddy. In the coastal eddy a mismatch between the physical and the biological centre was observed. The centre of the eddy defined by physical parameters (Stn 5) was a few kilometres east of the peak in phytoplankton. At this biological centre of the coastal eddy, depletion of nutrients had already occurred as a result of biological consumption. This illustrates the importance of relatively small-scale spatial variability in this area. In addition phytoplankton biomass and biodiversity of the oceanic eddy sampled at 24 h apart (i.e. Stns 1 and 2) were significantly different, suggesting a high temporal variability, even in a well-established water mass. Given such conditions, any single sample event represents a snapshot of the heterogeneity of the spring bloom in the separation zone of the EAC and more studies are required to fully reveal the spatial and temporal complexity of this area.

This study, however, brings several interesting findings and supports previous observations that eddies significantly affect phytoplankton biomass, biodiversity and productivity (Thompson et al., 2007). In this study, greater biomass was observed in both the oceanic and coastal eddy as compared with adjacent water masses (Stns 3, 4 and 6).. The primary productivity normalised per Chl *a* concentration was higher in the oceanic eddy than in the frontal zone of this eddy with the EAC, and in inner-shelf water.

4.2. Significance of eddies

Phytoplankton communities in mesoscale eddies can be quite distinct from both the inner-shelf communities where the eddy is formed and the background community in which the eddy systems are embedded (e.g., Ortner et al., 1979). For example, Jeffrey and Hallegraeff (1980) recorded greater species diversity with greater contribution of smaller cells (<15 μm) at the edge of a warm-core eddy, and higher biomass due to elevated diatom concentrations in its centre. Due to similarities of the phytoplankton communities (inferred using biomarker pigments) in coastal water and in the cold-core eddies (this study; Moore et al., 2007 for Western Australia), a coastal origin of the phytoplankton present inside the cold-core eddy is suggested. Our results support the hypothesis (Moore et al., 2007) that cold-core eddies represent an important mechanism to disperse phytoplankton offshore. This study showed a vertical nutrient supply in both eddies sampled, which could result in the greater biomass and different phytoplankton communities observed.

4.3. Significance of nutrients

Given that phytoplankton taxa have different nutrient requirements for growth (e.g., Sarthou et al., 2005; Schoemann et al., 2005; Veldhuis et al., 2005), then nutrients can affect the composition of the phytoplankton community (i.e. their biodiversity). Dissolved nutrient ratios in the various water masses studied were remarkably consistent, showing similar NO_3:Si and NO_3:PO_4 (Fig. 2 B). The ratio between NO_3:PO_4 equalled the Redfield ratio (16:1, slope 0.061, $r^2=0.98$, Redfield, 1958). The intercept was 0.02 μM PO_4, suggesting that NO_3 would be exhausted first if nutrients are consumed by phytoplankton according to the Redfield ratio. The NO_x and Si concentrations at ~200 m peaked at 18.3 and 7.0 μM, respectively. If consumed at 1:1 ratio, then silicate should run out first, leaving ~11 μM nitrate. Yet the nutrient consumption resulted in a non-zero ($p=0.005$) intercept of just 0.13 μM Si (Fig. 2B). Thus the realised consumption of NO_x and Si were significantly non-linear suggesting that diatoms must become a smaller proportion of the total community as nutrients are consumed and converted into phytoplankton biomass. This shift from diatoms to a more diverse phytoplankton community must occur during the spring nutrient drawdown.

Although total Chl *a* showed a clear spatial pattern, there was no direct relationship between dissolved nutrient concentrations and total Chl *a*. For example, the highest concentration of Chl *a* was observed in inner-shelf water but nutrients were lower than for other stations, presumably due to the different rates of nutrient supply and consumption, as opposed to total nutrient pools. In addition to nutrients, light is also essential for phytoplankton growth and may affect their vertical distribution and expression of specific pigments (e.g., Barlow et al., 2007).

The high Fv/Fm values observed suggested well-adapted, non (nutrient or light) limited phytoplankton communities. However, nutrient-enrichment experiments clearly demonstrated that nutrients have the ability to control phytoplankton abundance, biodiversity and total productivity in the separation zone of the EAC. Interestingly, nitrogen was the most limiting nutrient in water masses associated with the oceanic cold-core eddy. This is not surprising given that diatoms were not prevalent in this area. The nitrogen limitation of the phytoplankton community is known to have significant effect on phytoplankton composition. For example it could favour atmospheric nitrogen-fixing species (LaRoche and Breitbarth, 2005) already present in the Tasman Sea and the Coral Sea (e.g., Law et al., in review). In addition, the increasing temperature reported and predicted for the Tasman Sea (Ridgway, 2007; Hill et al., 2007; Hobday et al., 2006), will extend the area where temperature is above the threshold for *Trichodesmium* growth (18 °C)—a major nitrogen-fixing taxon (LaRoche and Breitbarth, 2005). Nitrate limitation can also affect the calcification of *Emiliania huxleyi* (Eek et al., 1999)—an important prymnesiophyte for carbon oceanic cycling that is present in the Tasman Sea. Finally, biological nitrogen limitation is intimately coupled with biological iron limitation. Both NO_3 reduction and atmospheric nitrogen fixation require iron (Sarthou et al., 2005; La Roche and Breitbarth, 2005; Law et al., in review). In fact, atmospheric nitrogen fixation by phytoplankton was found to be limited by iron in the Eastern Tasman Sea (Law et al., in review).

Previous research has suggested the potential for Si limitation in this region (Grant, 1971) but during the spring of 2008 nitrogen was far more limiting. It is possible that the importance of diatoms, previously reported in this area (Hallegraeff and Reid, 1986; Hallegraeff and Jeffrey, 1993), has declined as a result of prolonged decrease in Si concentrations below a threshold level, limiting for the growth of diatoms ($Si<0.6$ μM in 2006, Thompson et al., 2009). In fact, here no response of Si enrichment could be observed in coastal waters where concentrations of dissolved Si were above this threshold (1.6 μM Si).

Again this result may reflect the limited temporal sampling during a 2-week voyage and are likely not suitable for predicting long-term changes in nutrient or phytoplankton dynamics. As such, the results obtained here are associated with the understanding of seasonal nutrient limitation over a range of water masses that were all predominantly nitrogen limited. This study does not provide insights into long-term trends in diatom abundance in the separation zone of the EAC, and cannot determine whether the relatively few diatoms observed were the result of Si drawdown by diatoms at the earlier stage of the spring bloom.

4.4. Significance of biomarker pigments

To date, few studies of biomarker pigments have been made in this area. A larger scale review can be found in Thompson et al. (2011) showing consistent results for SE Australia. Barlow et al. (2007) also used biomarkers to differentiate between three groups of phytoplankton: diatoms, small flagellates and prokaryotes. Along a 30°S transect off east Australia they observed a greater abundance of flagellates. Prokaryotes were increasing eastwards of Australia, with greater abundances relative to diatoms east of ~155°E. Here HPLC biomarkers showed contrasting phytoplankton populations in different water masses, suggesting they could be used to assess the biological signature of water masses in the separation zone of the EAC. Marked differences were also observed vertically with significant contrasts between the surface water and the Chlmax. The EAC water was characterised by relatively low Chl *a* phytoplankton biomass and unique presence of prochlorophytes (DV Chl *a* and *b*). Cyanophytes were only found in the oceanic eddy and the EAC. Chlorophytes were important only in inner-shelf waters including the coastal eddy and diatoms dominated closer inshore at ~33.5°S. Further south where the spring bloom had barely

commenced, phytoplankton biomass was generally low and high surface nutrients were still present. Prymnesiophytes (19hex), probably coccolithophorids, were ubiquitous in the region as were pelagophytes (19but). Both these picoeukaryotes are found widespread throughout the tropical Pacific (Andersen, 1985; Landry et al. 1996). As observed in the separation zone of the EAC during spring 2008, they are often found near the bottom of the euphotic zone. Pelagophytes in particular are regularly identified via pigments (Suzuki et al. 1997; DiTullio et al. 2003; Marty et al., 2008) and can represent 40% of the picoeukaryotes at the Chlmax (Not et al., 2008).

To refine our understanding on the dynamic and the parameters that control phytoplankton community in this area, both interconnection of biogeochemical cycles (nitrogen and iron) and variable biological requirement need to be considered. Long-term trends in the strength of the South Pacific gyre will influence the flow of the EAC through this region (Hill et al. 2007) impacting on biogeochemical cycling (Thompson et al., 2009). Seasonal factors such as development of a relatively deep mixed layer in winter (Condie and Dunn, 2006) annually resupplying the euphotic zone with dissolved inorganic nutrients are influencing the phytoplankton ecology of the region. Processes such as increased insolation and declining wind stress that cause shallowing of the mixed-layer depth in spring must be important in the timing and magnitude of the resulting spring bloom (Baird et al., 2006). The development of frontal zones, upwellings and eddies create mesoscale and submesoscale variation that remains poorly understood. In addition, temperature and especially grazing can effectively control the phytoplankton community. Finally, because of the difference in the timescale of the change in physical oceanography and the initiation of an associated biological response, studies following temporal variability as biological responses develop, and other Lagrangian-type investigations are required.

Acknowledgments

The authors warmly thank Iain Suthers and Mark Baird for the opportunity to join their research voyage: "Salps and eddies" on the *R.V. Southern Surveyor*. We also thank the Marine National Facility team for their support, including the captain and crew of the *R.V. Southern Surveyor*, Pru Bonham and Lesley Clementson (CSIRO) for pigment analyses, and Peter Oke (CSIRO) for satellite images. CSH was supported by a CSIRO Post-doctoral Fellowship and RD by a UTS C3 honours scholarship. This is SIMS publication number 0040.

References

Andersen, V., 1985. Filtration and ingestion rates of *Salpa Fusiformis* Cuvier (Tunicata: Thaliacea): effects of size, individual weight and algal concentration. J. Exp. Mar. Biol. Ecol. 87, 13–29.

Baird, M.E., Timko, P.G., Suthers, I.M., Middleton, J.H., 2006. Coupled physical–biological modelling study of the East Australian Current with idealised wind forcing. Part I: biological model intercomparison. J. Mar. Syst. 59, 249–270.

Baird, M.E., Timko, P.G., Middleton, J.H., Mullaney, T.J., Cox, D.R., Suthers, I.M., 2008. Biological properties across the Tasman Front off southeast Australia. Deep-Sea Res. I 55, 1438–1455.

Baird, M.E., Everett, J.D., Suthers, I.M., 2011. Analysis of southeast Australian zooplankton observations of 1938-42 using synoptic oceanographic conditions. Deep-Sea Res. II 58, 699–711.

Bakun, A., 2006. Fronts and eddies as key structures in the habitat of marine fish larvae: opportunity, adaptive response and competitive advantage. Scientia Marina 70S2, 105–122.

Barlow, R.G., Mantoura, R.F.C., Gough, M.A., Fileman, T.W., 1993. Pigment signatures of the phytoplankton composition in the northeastern Atlantic during the 1990 spring bloom. Deep-Sea Res. II 40, 459–477.

Barlow, R.G., Stuart, V., Lutz, V., Sessions, H., Sathyendranath, S., Platt, T., Kyewalyanga, M., Clementson, L., Fukasawa, M., Watanage, S., Devred, E., 2007. Seasonal pigment patterns of surface phytoplankton in the subtropical Southern hemisphere. Deep-Sea Res. I 54, 1687–1703.

Booth, D.J., Figueira, W.F., Gregson, M.A., Brown, L., Beretta, G., 2007. Occurrence of tropical fishes in temperate south-eastern Australia: role of the East Australia Current. East. Coast. Shelf Sci. 72 (1–2), 102–114.

Condie, S.A., Dunn, J.R., 2006. Seasonal characteristics of the surface mixed layer in the Australasian region: implications for primary production regimes and biogeography. Mar. Freshwater Res. 57, 569–590.

Cowley, R., Critchley, G., Eriksen, R., Latham, V., Plaschke, R., Rayner, M., Terhell, D., 1999. CSIRO Marine Laboratories Report 236 Hydrochemistry Operations Manual. Tech. rep., CSIRO Marine Laboratories, Hobart.

Cresswell, G., 1994. Nutrient enrichment of the Sydney continental shelf. Aust. J. Mar. Freshwater Res. 45, 677–691.

DiTullio, G.R., Geesey, M.E., Jones, D.R., Daley, K.L., Campbell, L., Smith Jr, W.O., 2003. Phytoplankton assemblage structure and primary productivity along 1708W in the South Pacific Ocean. Mar. Ecol. Prog. Ser. 255, 55–80.

Eek, M.K., Whiticar, M.J., Bishop, J.K.B., Wong, C., 1999. Influence of nutrients on carbon isotope fractionation by natural populations of Prymnesiophyte algae in NE Pacific. Deep-Sea Res. II 46, 2863–2876.

Godfrey, J.S., Cresswell, G.R., Golding, T.J., Pearce, A.F., Boyd, R., 1980b. The separation of the East Australian Current. J.Phys. Oceanogr. 10, 430–440.

Goericke, R., Repeta, D.J., 1992. The pigments of Prochlorococcus marinus—the presence of divinyl chlorophyll-*a* and chlorophyll-*b* in a marine prokaryote. Limnol. Oceanogr. 37, 425–433.

Grant, B.R., 1971. Variation in silicate concentration at Port Hacking station, Sydney, inrelation to phytoplankton growth. Aust. J. Mar. Freshwater Res. 22, 49–54.

Hallegraeff, G.M., 1981. Seasonal study of phytoplankton pigments and species at a coastal station off Sydney: importance of diatoms and the nanoplankton. Mar. Biol. 61, 107–118.

Hallegraeff, G.M., Reid, D.D., 1986. Phytoplankton species successions and their hydrological environment at a coastal station off Sydney. Aust. J. Mar. Freshwater Res. 37, 361–377.

Hallegraeff, G.M., Jeffrey, S.W., 1993. Annually recurrent diatom blooms in spring along the New South Wales coast of Australia. Aust. J. Mar. Freshwater Res. 44, 325–334.

Hassler, C.S., Schoemann, V., 2009. Bioavailability of organically bound iron in controlling Fe to model phytoplankton of the Southern Ocean. Biogeosci. Discuss. 6, 1677–1712 Special issue Iron biogeochemistry across marine systems at changing times.

Hill, K.L., Rintoul, S.R., Coleman, R., Ridgway, K.R., 2007. Wind forced low frequency variability of the East Australia Current. Geophys. Res. Lett., 35, L08602, 10.1016/j.dsr2.2010.06.008.

Hobday, A.J., Okey, T.A., Poloczanska, E.S., Kunz, T.J., Richardson, A.J., 2006. Impacts of climate change on Australian marine life: Part B. Technical Report, Report to the Australian Greenhouse Office, Canberra, Australia.

Jassby, A.D., Platt, T., 1976. Mathematical formulation of the relationship between photosynthesis and light for phytoplankton. Limnol. Oceanogr. 21, 540–547.

Jeffrey, S.W., Hallegraeff, G.M., 1980. Studies of phytoplankton species and photosynthetic pigments in a warm core eddy of the East Australian Current. I. Summer populations. Mar. Ecol. Prog. Ser. 3, 285–294.

Jeffrey, S.W., Mantoura, R.F.C., Wright, S.W. (Eds.), 1997. Phytoplankton Pigments in Oceanography: Guidelines to Modern Methods Monographs on Oceanographic Methodology. UNESCO Publishing.

Landry, M.R., Kirshtein, J., Constantinou, J., 1996. Abundances and distributions of picoplankton populations in the central equatorial Pacific from 12°N to 12°S, 140°W. Deep-Sea Res. II 43, 871–890.

LaRoche, J., Breitbarth, E., 2005. Importance of the diazothrophs as a source of new nitrogen in the ocean. J. Sea Res. 53, 67–91.

Law, C.S., Ellwood, M. Marriner, A., Woodward, E.M.S. Gradients and controls of nitrogen fixation in the south-west Pacific. Global Biogeochem. Cycles, in review.

Mann, K.H., Lazier, J.R.N., 2006. Dynamics of Marine Ecosystems third ed. Blackwell Scientific Publications Inc., Oxford.

Mantoura, R.E.C., Llewellyn, C.A.N., 1983. The rapid determination of algal chlorophyll and carotenoid pigments and their breakdown products in natural waters by reversed-phase high-performance liquid chromatography. Anal. Chim. Acta 151, 297–314.

Marty, J.C., Garcia, N., Raimbault, P., 2008. Phytoplankton dynamics and primary production conditions in the NW Mediterranean Sea. Deep-Sea Res. I 55, 1131–1149.

McLean-Padman, J., Padman, L., 1991. Summer upwelling on the Sydney inner continental shelf: the relative roles of local wind forcing and mesoscale eddy encroachment. Cont. Shelf Res. 11, 321–345.

Moore, T.S., Matear, R.J., Marra, J., Clementson, L., 2007. Phytoplankton variability off the Western Australian Coast: mesoscale eddies and their role in cross-shelf exchange. Deep Sea Res. II 54, 943–960.

Nilsson, C.S., Cresswell, G.R., 1981. The formation and evolution of East Australian Current warm-core eddies. Prog. Oceanogr. 9, 133–183.

Newell, B.S., 1996. Seasonal changes in the hydrological and biological environments off Port Hacking, Sydney. Aust. J. Mar. Freshwater Res. 17, 77–91.

Not, F., Latasa, M., Scharek, R., Viprey, M., Karleskind, P., Balague, V., Ontoria-Oviedo, I., Cumino, A., Goetze, E., Vaulot, D., Massana, R., 2008. Protistan assemblages across the Indian Ocean, with a specific emphasis on the picoeukaryotes. Deep Sea Res. I 55, 1456–1473.

Oke, P.R., Middleton, J.H., 2000. Topographically induced upwelling off Eastern Australia. J. Phys. Oceanogr. 30, 512–531.

Oke, P.R., Middleton, J.H., 2001. Nutrient enrichment off port stephens: the role of the East Australian Current. Cont. Shelf Res. 21, 587–606.

Ortner, P.B., Hulbert, E.M., Wiebe, P.H., 1979. Phytohydrography, Gulf Stream rings, and herbivore habitat contrasts. J. Exp. Mar. Biol. Ecol. 39, 101–124.
Redfield, A.C., 1958. The biological control of chemical factors in the environment. Am. Sci. 46, 205–221.
Ridgway, K.R., Godfrey, J.S., 1997. Seasonal cycle of the East Australian Current. J. Geophys. Res. 102, 22921–22936.
Ridgway, K.R., 2007. Long-term trend and decadal variability of the southward penetration of the East Australian current. Geophys. Res. Lett. 34, L13612. doi:10.1029/2007GL030393.
Ridgway, K., Hill, K., 2009. The East Australian Current. In: Poloczanska, E.S., Hobday, A.J., Richardson, A.J. (Eds.), A Marine Climate Change Impacts and Adaptation Report Card for Australia 2009, 05/09. NCCARF Publication, pp. 1–16.
Roughan, M., Middleton, J.H., 2002. A comparison of observed upwelling mechanisms off the east coast of Australia. Cont. Shelf Res. 22, 2551–2572.
Roughan, M., Middleton, J.H., 2004. On the East Australia Current: variability, encroachment, and upwelling. J. Geophys. Res. 109, C07003.
Sarthou, G., Timmermans, K.R., Blain, S., Treguer, P., 2005. Growth physiology and fate of diatoms in the ocean: a review. J. Sea Res. 53, 25–42.
Schoemann, V., Becquevort, S., Stefels, J., Rousseau, V., Lancelot, C., 2005. *Phaeocystis* blooms in the global ocean and their controlling mechanisms: a review. J. Sea Res. 53, 43–66.
Suzuki, K., Handa, N., Kiyosawa, H., Ishizaka, J., 1997. Temporal and spatial distribution of phytoplankton pigments in the Central Pacific Ocean along 175°E during the Boreal Summers of 1992 and 1993. J. Oceanogr. 53, 383–396.
Thompson, P.A., Pesant, S., Waite, A.M., 2007. Contrasting the vertical differences in the phytoplankton biology of a dipole pair of eddies in the south-eastern Indian Ocean. Deep-Sea Res. II, 1003–1028.
Thompson, P.A., Baird, M.E., Ingleton, T., Doblin, M.A., 2009. Long-term changes in temperate Australian coastal waters: implications for phytoplankton. 394, 1-19, 10.3354/meps08297.
Thompson, P.A., Bonham, P.B., Waite, A.M., Clementson, L.A., Cherukuru, N., Doblin, M.A., 2011. Contrasting oceanographic conditions and phytoplankton communities on the east and west coasts of Australia 58, 645–663.
Tilburg, C.E., Hurlburt, H.E., O'Brien, J.J., Shriver, J.Y., 2001. The dynamics of the East Australian current system: the Tasman Front, the East Auckland Current, and the East Cape Current. J. Phys. Oceanogr. 31, 2917–2943.
Tranter, D.J., Carpenter, D.J., Leech, G.S., 1986. The coastal enrichment effects of the East Australian Current eddy field. Deep-Sea Res. 33, 1705–1728.
van Heukelem, L., Thomas, C., 2001. Computer assisted high-performance liquid chromatography method development with applications to the isolation and analysis of phytoplankton pigments. J. Chromatogr. A. 910, 31–49.
Veldhuis, M.J.W., Timmermans, K.R., Croot, P., van der Wagt, B., 2005. Picoplankton; a comparative study of their biochemical composition and photosynthetic properties. J. Sea Res. 53, 7–24.